

## Spatially Regulated Expression of Homeotic Genes in *Drosophila*

Katherine Harding, Cathy Wedeen  
William McGinnis, Michael Levine

A fundamental problem of development is how embryonic cells acquire their particular developmental fates as a result of their location within a developing embryo. A model system for analyzing the elaboration of this positional information during *Drosophila* development involves the morphogenesis of body segments. The adult fruit fly is composed of eight abdominal, three tho-

dermal tissues of the affected segment as well (2, 3, 7). For example, embryos that lack the *Antennapedia* (*Antp*) gene function display a transformation of the meso- and metathorax (T2 + T3) into homologous tissues of the prothorax (T1) (8).

Many homeotic genes appear within one of two clusters in the *Drosophila* genome, the bithorax complex (BX-C)

---

**Abstract.** *The sites of transcript accumulation for six different homeotic loci of the Antennapedia and bithorax gene complexes (ANT-C and BX-C) were identified within embryo tissue sections by in situ hybridization. These six loci belong to the Antennapedia class of the homeo box gene family. Transcripts encoded by each locus are detected primarily in discrete, nonoverlapping regions of the embryonic central nervous system (CNS). The regions of the CNS that contain transcripts encoded by each of these loci correspond to the embryonic segments that are disrupted in mutants for these genes. The maintenance of spatially restricted expression of each ANT-C and BX-C locus could involve hierarchical, cross-regulatory interactions that are mediated by the homeo box protein domains encoded by these genes.*

---

racic, and four to six head segments (1). Several of the constituent tissues of a given segment have morphological properties specific for that segment. For example, the epidermis elaborates cuticular structures, such as legs and antennae, that are distinct for a particular segment. In addition, the morphology of some of the mesodermal (2) and neural tissues (3, 4) may be specific for a given segment.

Homeotic genes are those that establish the diverse pathways by which each embryonic segment primordium develops a distinct adult phenotype (5, 6). Mutations of homeotic loci result in partial or complete transformations of the epidermal tissues of one segment into those of another. Homeotic transformations may include the neural and meso-

(5, 9) or the Antennapedia complex (ANT-C) (10, 11). Genes of the BX-C are required for the specification of segments in the posterior regions of the fly (5, 12, 13). Lewis has identified a number of homeotic loci within the BX-C on the basis of embryonic and adult mutant phenotypes (5). Recently, a minimum of three essential domains of homeotic function within the BX-C have been identified by means of lethal complementation analyses: *Ultrabithorax* (*Ubx*), *Abdominal-A* (*abd-A*), and *Abdominal-B* (*Abd-B*) (9). The ANT-C is required for the specification of anterior body segments (8, 14). Several homeotic lethal complementation groups have been identified for the ANT-C (8, 11, 14, 15). These include the *Antp*, *Sex combs reduced* (*Scr*), and *Deformed* (*Dfd*) loci. Each ANT-C and BX-C homeotic lethal complementation group controls the development of a different subset of the embryonic segment primordia (Fig. 1a).

A central problem in elucidating the genetic control of segment morphogenesis is how the different ANT-C and BX-C loci come to function in primarily nonoverlapping domains along the body axis of the fly. The molecular cloning of ANT-C and BX-C loci has permitted a direct assessment of the spatial and temporal limits of homeotic gene expression. The previous demonstration that *Ubx* and *Antp* share direct nucleotide sequence homology (16-19) facilitated the isolation of ANT-C and BX-C loci. This homology occurs within a conserved protein coding region designated the homeo box. A total of seven genomic DNA fragments cross-hybridizes strongly with the *Antp* and *Ubx* homeo boxes (20). These seven regions correspond to the Antennapedia class of the homeo box gene family, all of which are located within either the ANT-C or the BX-C (20). It appears that each of the six lethal complementation groups of the ANT-C and BX-C (Fig. 1) contains an Antennapedia class homeo box. However, there are additional homeotic loci within the BX-C that do not contain the homeo box (Fig. 1a) (21).

We show that each of the ANT-C and BX-C homeotic loci that contains a homeo box specifies transcripts that accumulate in discrete regions of the embryonic central nervous system (CNS). To a close approximation, the regions of the CNS that contain transcripts encoded by each of these loci correspond to the embryonic segments that are disrupted in mutants for these genes. We propose that spatially restricted expression of each ANT-C and BX-C locus involves hierarchical, cross-regulatory interactions that are mediated by the homeo box protein domains encoded by these genes. Support for this model is based on analysis of the distribution patterns of *Antp* transcripts in mutant embryos that lack BX-C loci.

**Isolation of a new ANT-C homeo box locus.** Molecular clones for the *Dfd*, *Antp*, *Ubx*, *iab-2*, and *iab-7* loci have been previously isolated (16, 20, 22-25). In order to determine the spatial limits of expression for each homeotic lethal complementation group within the ANT-C and BX-C by in situ hybridization, it was necessary to obtain a molecular probe for the *Scr* locus. A genomic DNA fragment that appears to derive from *Scr* was isolated on the basis of homeo box sequence homology as described below.

A total of  $6 \times 10^4$  recombinants from a *Drosophila*-Charon 4 DNA library (approximately six genome equivalents) were screened with the homeo box se-

---

K. Harding, C. Wedeen, and M. Levine are in the Department of Biological Sciences, Fairchild Center, Columbia University, New York 10027. W. McGinnis is in the Department of Molecular Biophysics and Biochemistry, Yale University, New Haven, Connecticut 06520.

quence as described (16). Approximately 50 cross-hybridizing recombinant phage were isolated. By in situ hybridization to polytene chromosomes, clone A40 was found to reside within the 84A/B cytogenetic region of chromosome 3. Previous cytogenetic analyses have demonstrated that this corresponds to the location of the ANT-C (11). As judged by high stringency cross-hybridization tests, A40 does not correspond to the previously isolated *Dfd*, *fushi tarazu* (*ftz*), and *Antp* loci.

The *Scr* locus has been mapped to a region of the ANT-C that lies between the *Dfd* and *Antp* loci (14, 15, 24). Mutant embryos that lack *Scr* function show homeotic transformations of the posterior-most head regions (the labium) and the prothorax (8, 14). Since *Dfd* and *Antp* transcripts principally accumulate in the regions of the CNS corresponding to the embryonic segments that are most disrupted in *Dfd*<sup>-</sup> and *Antp*<sup>-</sup> mutants (16, 26, 27, see below), we anticipated that *Scr* transcripts would be detected in the embryonic subesophageal ganglion.

To determine the time during embryonic development when A40 is transcribed, we hybridized Northern blots containing polyadenylated [poly(A)<sup>+</sup>] RNA from successive embryonic stages with the homeo box region of the A40 clone. Multiple RNA species homologous to pA40 are found during embryonic development, especially in 6- to 12-hour embryos (Fig. 2). The largest transcript is 4.0 kb in length. In situ hybridization analyses (see below) confirm that mid-stage embryos contain the highest levels of A40 transcript. In addition, A40 transcripts are primarily detected within tissues of the labial head segment. Since A40 maps within the 84A/B cytogenetic interval, contains homeo box cross-homology, and is expressed in the embryonic segment most disrupted in *Scr*<sup>-</sup> mutants (8, 14), it is likely that A40 derives from the *Scr* locus of the ANT-C (28).

**ANT-C and BX-C gene expression in wild-type embryos.** The regions of developing embryos that accumulate transcripts specified by *Antp* and *Ubx* have been identified by in situ hybridization to tissue sections (26, 27, 29). The principal sites of *Antp*<sup>+</sup> and *Ubx*<sup>+</sup> expression appear to correspond to the embryonic segments that are most severely disrupted in *Antp*<sup>-</sup> and *Ubx*<sup>-</sup> mutants. For the most part, *Antp* transcripts accumulate in the T1/T2 portion of the embryonic CNS (26, 27, 30). *Ubx* transcripts are detected principally in T3/A1 (29).

The identities of tissues that contain

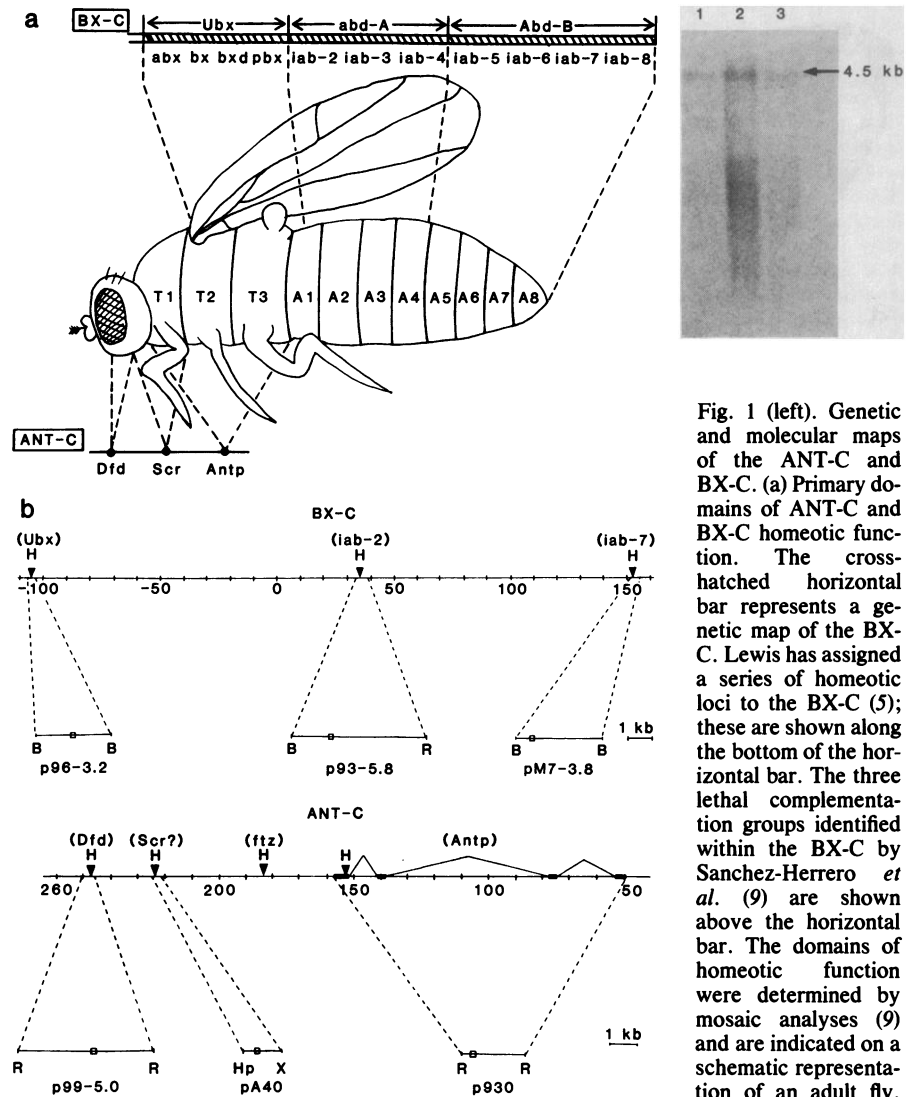


Fig. 1 (left). Genetic and molecular maps of the ANT-C and BX-C. (a) Primary domains of ANT-C and BX-C homeotic function. The cross-hatched horizontal bar represents a genetic map of the BX-C. Lewis has assigned a series of homeotic loci to the BX-C (5); these are shown along the bottom of the horizontal bar. The three lethal complementation groups identified within the BX-C by Sanchez-Herrero *et al.* (9) are shown above the horizontal bar. The domains of homeotic function were determined by mosaic analyses (9) and are indicated on a schematic representation of an adult fly. *Ubx* is critically required for the develop-

ment of the posterior compartment of the mesothorax (T2p) (39) through the anterior compartment of the first abdominal segment (A1a). The *abd-A* function is required for morphogenesis of A1p through A4, and *Abd-B* is required for A5, through A8. The relationship between the Lewis (5) and Sanchez-Herrero *et al.* (9) genetic maps is uncertain. An approximate correlation is indicated by the horizontal arrows associated with each lethal complementation group. At least three essential homeotic functions have been assigned to the ANT-C: *Dfd*, *Scr*, and *Antp*. These are shown on the genetic map below the schematic of the fly. The primary domains of ANT-C function are indicated. *Antp* function is required for proper segment morphogenesis of the thorax (8, 33, 44). Analyses of *Scr*<sup>-</sup> and *Dfd*<sup>-</sup> mutant embryos suggest that these genes are required for the differentiation of the prothorax and posterior head regions (8, 14). (b) Molecular maps of the BX-C and the ANT-C. The horizontal lines correspond to overlapping cloned genomic DNA's that span the two complexes [for details see (20, 22-24, 38); units are kilobase pairs]. Arrowheads indicate the positions of homeo box copies within the two complexes. Homeo box-containing cloned genomic DNA's used as probes for in situ hybridizations are indicated below the horizontal lines; the positions within the chromosome walk from which these cloned DNA's are derived are indicated by the connecting dashed lines. The open boxes within each cloned DNA used as a probe correspond to the position of the homeo box within each fragment. The *ftz* homeo box region was not used in this analysis. The probe p99-5.0 is a 5-kb Eco RI genomic DNA fragment that derives from the *Dfd* locus; pA40 is a 1.4-kb Hpa I-Xho I genomic fragment that appears to derive from the homeo box region of the *Scr* locus (the exact position of the homeo box within the fragment has not been determined); p903 is a 2.3-kb *Antp* cDNA; p96-3.2 is a 3.2-kb Bam HI genomic fragment with homology to *Ubx* transcripts; p93-5.8 is a 5.8-kb Bam HI-Eco RI genomic fragment with homology to *iab-2* transcripts; pM7-3.8 is a 3.8-kb Bam HI genomic fragment with homology to *iab-7* transcripts (20, 38). Fig. 2 (right). Transcripts homologous to the putative *Scr* probe. Poly(A)<sup>+</sup> RNA was extracted from wild-type embryos, and 10- $\mu$ g aliquots were fractionated on an agarose-formaldehyde gel and transferred to nitrocellulose (20). The lanes in each panel correspond to embryonic stages 1 (0 to 6 hours), 2 (6 to 12 hours), and 3 (12 to 24 hours). The blot was hybridized with the pA40 DNA fragment (Fig. 1b) after labeling with <sup>32</sup>P by nick-translation; nonspecifically bound probe was removed by stringent washing. The strongest hybridization signal (arrow) corresponds to a poly(A)<sup>+</sup> RNA species 4.0 kb in length. Autoradiographic exposure was for 10 days.

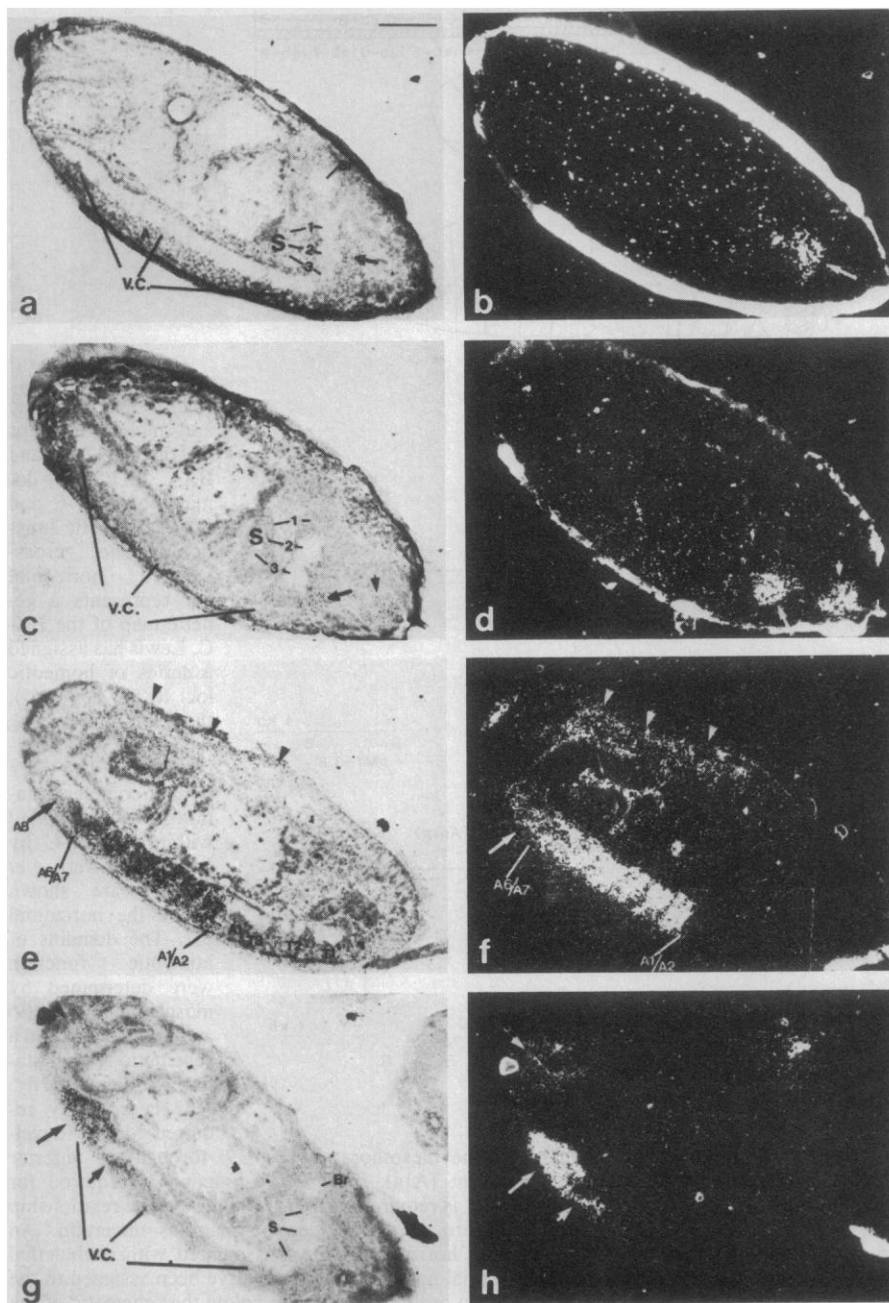


Fig. 3. Localization of *Dfd*, *Scr*, *iab-2*, and *iab-7* transcripts in 12- to 14-hour embryos. All sections are sagittal and are oriented such that anterior is to the right and dorsal is up. Because of this orientation, the left-to-right order of the body segments shown in each photomicrograph is opposite to the order in which the labels are read. For example, in a region labeled T1/T2, T1 is actually to the right (more anterior) of T2 in the tissue autoradiogram. The luminescence of the chorion in darkfield photomicrographs is due to refraction of light and does not indicate nonspecific or specific hybridization. The bar in (a) represents 0.1 mm. (a) Localization of transcripts homologous to the *Dfd* probe (p99-5.0). Hybridization signals are seen over the cells of the S1/S2 region of the subesophageal ganglion (arrow). No signals over background are detected in regions either anterior or posterior to S1/S2. (b) Dark-field photomicrograph of the same section as in (a). (c) Localization of transcripts homologous to the putative *Scr* probe, pA40. Hybridization signals are seen over the S2/S3 region of the subesophageal ganglion (arrow); hybridization is also seen to labial tissues (arrowhead). No other sites of hybridization are detected. (d) Dark-field photomicrograph of the same section as in (c). (e) Localization of transcripts homologous to the *iab-2* probe. The strongest hybridization signals occur over A1/A2 through A6/A7 ventral ganglia. Weaker signals are observed in the A8 ganglion (arrow) as well as in the hypodermal and mesodermal regions of segments A2 through A6/A7 (arrowheads). (f) Dark-field photomicrograph of the same section as in (e). (g) Localization of transcripts homologous to the *iab-7* probe. The strongest hybridization signals are seen in the A6/A7 and A8/A9 ventral ganglia (large arrow); weaker hybridization is observed in A5/A6 (small arrow) and in hindgut tissues (arrowhead). (h) Dark-field photomicrograph of the same section as in (g). Abbreviations: A, abdominal region of the ventral cord; Br, brain; S, subesophageal ganglion; T, thoracic region of the ventral cord; v.c., ventral cord.

*Dfd*, *Scr*, *iab-2*, and *iab-7* RNA's were determined by an in situ hybridization technique (26). Serial tissue sections of wild-type embryos at various stages of development were separately hybridized to tritium-labeled genomic DNA fragments that contain a homeo box (Fig. 1b). A primary site of hybridization for each of these probes corresponds to neural tissues.

The embryonic CNS is composed of the dorsally located brain, which is connected to a ventral nerve cord by a subesophageal ganglion. The ventral cord is a composite of 11 repeating ganglia each of which contains approximately 300 nerve cells (31). The epidermal portions of each of the three thoracic and eight abdominal segments are innervated by a corresponding ganglion of the ventral cord.

At mid-embryonic stages, *Dfd* transcripts are detected in a central portion of the subesophageal ganglion, S1/S2 (Fig. 3, a and b). Transcripts homologous to the putative *Scr* probe, pA40, are detected in the S2/S3 region of the subesophageal ganglion of mid-stage embryos. A second focus of embryonic hybridization is observed over epidermal and mesodermal tissues of a posterior head segment, probably the labium (Fig. 3, c and d).

Strong *iab-2* hybridization signals are detected in the A1/A2 through the A6/A7 ventral ganglia of mid-stage embryos. Less labeling is observed in the posterior-most ventral ganglia (Fig. 3, e and f). RNA's homologous to the *iab-7* hybridization probe are detected primarily in the posterior-most ventral ganglia, including at least a posterior portion of the A7 ganglion and all of the composite A8/A9 ganglion. Less intense hybridization signals are observed over the A5 and A6 ventral ganglia (Fig. 3, g and h).

Germ band extension occurs approximately 5 hours after fertilization (31). During this time, the ectodermal and mesodermal cell layers that lie along the ventral aspect of the embryo expand posteriorly. About 7 to 8 hours after fertilization the germ band begins to retract to its original site of formation. It is during germ band extension and retraction when the ectodermally derived neuroblasts differentiate and subsequently elaborate ganglion cells by undergoing unequal mitotic divisions (31).

Embryos undergoing elongation of the germ band were hybridized with the cloned *Dfd*, A40, and *Antp* homeo box regions of the ANT-C. The *Dfd* probe principally hybridizes to the mesodermal, neural, and epidermal progenitors of a posterior head segment—possibly

Fig. 4 (upper right). Localization of *Dfd*, *A40*, and *Antp* transcripts during germ band extension. The orientation of the sections and other features of presentation are as described in the legend of Fig. 3. The bar in (a) corresponds to 0.1 mm. (a) Localization of transcripts homologous to the *Dfd* probe. The strongest hybridization signals are seen in the region that gives rise to the S1/S2 region of the subesophageal ganglion and portions of the maxilla (arrow); signals are also detected in cells which appear to correspond to a more anterior region of the presumptive head (arrowheads). (b) Dark-field photomicrograph of the same section as in (a). (c) Localization of transcripts homologous to the putative *Scr* probe, pA40. Hybridization signals are detected in two regions of the presumptive ventral cord, one of which gives rise to S2/S3 (arrows). (d) Dark-field photomicrograph of the same section as in (c). (e) Localization of transcripts homologous to the *Antp* probe (p903). Strong hybridization signals are seen over the regions giving rise to S3/T1, T1/T2, and T2/T3; weaker hybridization signals are seen more posteriorly through A8. (f) Dark-field photomicrograph of the same section as in (e). Abbreviations: AMG, anterior midgut invagination; gb, germ band; PMG, posterior midgut invagination; St, stomadeum.

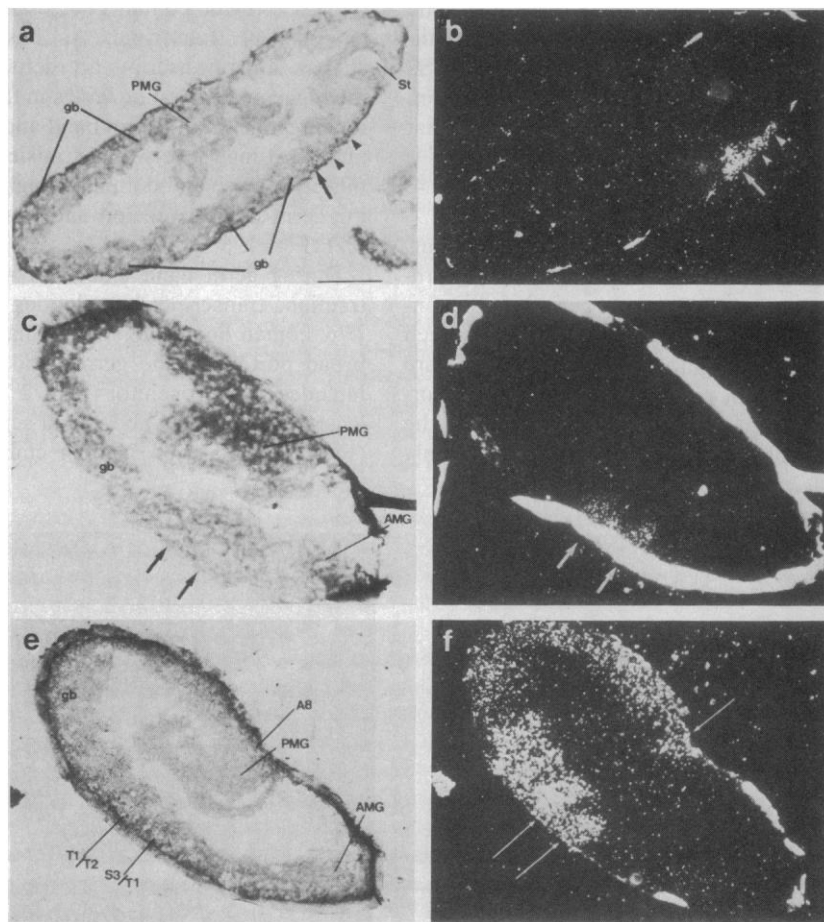
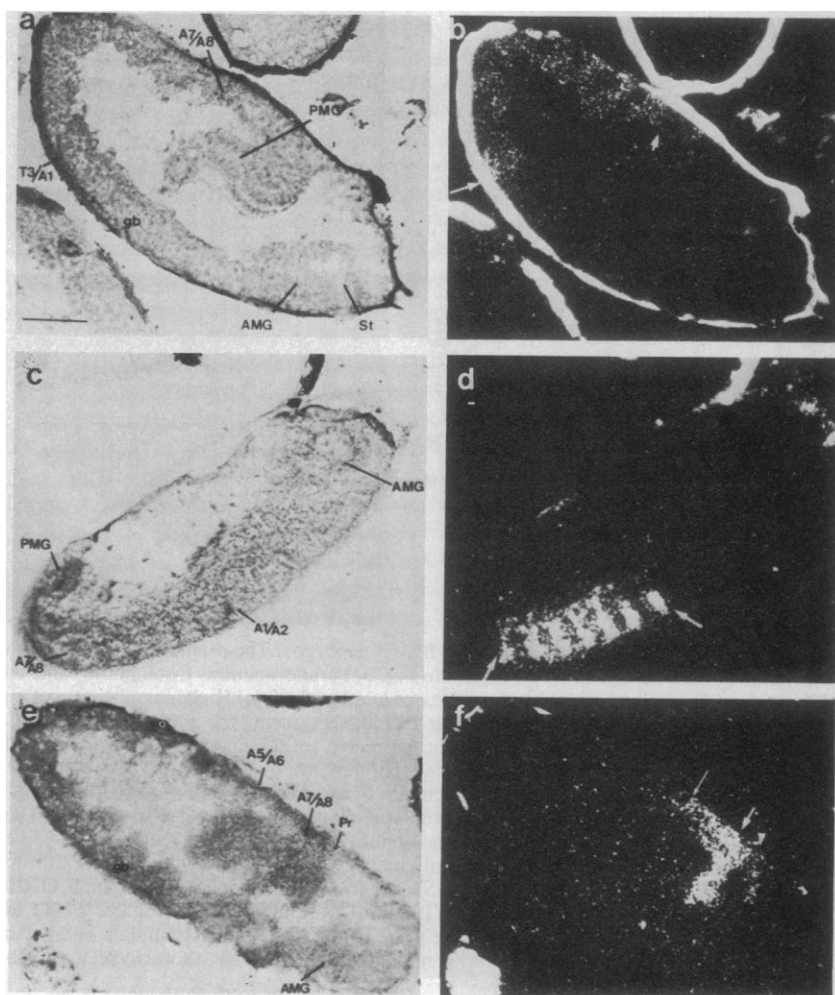


Fig. 5 (lower right). Localization of *Ubx*, *iab-2*, and *iab-7* transcripts during germ band extension and retraction. The orientation of the sections and other features are as described in the legend to Fig. 3. The bar in (a) represents 0.1 mm. (a) Localization of transcripts homologous to the *Ubx* probe in an embryo undergoing germ band extension. Hybridization signals are detected over regions corresponding to the presumptive T2/T3 → A7/A8 segments. (b) Dark-field photomicrograph of the same tissue section as in (a). Arrows demarcate T2/T3 → A7/A8. (c) Localization of transcripts homologous to the *iab-2* probe in an embryo undergoing germ band retraction. Intense hybridization signals are seen in regions corresponding to A1/A2 → A6/A7 with slightly weaker signals seen in A7/A8. (d) Dark-field photomicrograph of the same section as in (c); arrows bracket A1/A2 → A7/A8. (e) Localization of transcripts homologous to the *iab-7* probe in an embryo with a fully extended germ band. Strong hybridization signals are detected in the regions corresponding to A7 and A8. Weaker hybridization signals are detected in regions anterior to A7 in a graded fashion with A7/A8 showing the strongest intensity of hybridization and A5/A6 the weakest. Weak hybridization is also detected in a region posterior to A8; this region might correspond to future hindgut structures. (f) Dark-field photomicrograph of the same section as in (e). Thick arrow indicates A8; thin arrow indicates A5/A6; arrowhead indicates possible hindgut labeling. Abbreviations: AMG, anterior midgut invagination; gb, germ band; PMG, posterior midgut invagination; Pr, proctodeum; St, stomadeum.



the maxilla (Fig. 4, a and b, arrows). The neural tissues of this segment primordium appear to give rise to the S1/S2 region of the subesophageal ganglion. Weaker labeling is also observed at what might be the epidermal portions of a more anterior region of the head (Fig. 4, a and b, arrowheads).

A40 transcripts appear to be distributed over a broader portion of the presumptive CNS during germ band extension as compared with more advanced stages of neurogenesis. Transcripts are present in two distinct segment primordia (Fig. 4, c and d); however, at the conclusion of germ band retraction, only

the S2/S3 region contains detectable levels of A40 transcripts. As has been shown, *Antp* transcripts are detected at the highest steady-state levels in the thoracic regions of the germ band and accumulate at high levels only transiently in the presumptive abdominal ganglia during germ band extension and retraction (27) (Fig. 4, e and f).

During germ band extension and retraction, transcripts homologous to the *Ubx* homeo box region accumulate in a broad portion of the germ band which includes the progenitors of T2 and at least the first seven abdominal segments (Fig. 5, a and b). At similar embryonic

stages, *iab-2* transcripts are detected in the A1/A2 through A7/A8 regions of the germ band (Fig. 5, c and d). During germ band extension, *iab-7* transcripts are detected primarily in the A6/A7, A7/A8, and A8/A9 segments. In addition, weak hybridization is observed to more anterior segments, including A4/A5. Weak hybridization is also observed to a region posterior to the A8/A9 segments, possibly including presumptive hindgut structures (Fig. 5, e and f).

**Altered distribution of *Antp*<sup>+</sup> transcripts in BX-C<sup>-</sup> embryos.** BX-C<sup>-</sup> embryos [Df(3R)P9 homozygotes] die during the terminal stages of embryogenesis (5). Lewis has shown that the epidermal tissues of embryonic segments T3 through A7 acquire features characteristic of the mesothorax (T2). More recently, it has been suggested that each of the transformed segments might acquire a composite pro- and mesothoracic (T1/T2) identity (32, 33). In advanced stage BX-C<sup>-</sup> embryos, *Antp*<sup>+</sup> transcripts persist at high steady-state levels in the region of the ventral cord that encompasses the T1/T2, T3, and first seven abdominal ganglia (34).

*Antp* transcripts are detected in the T1/T2 and T2/T3 segment primordia of BX-C<sup>-</sup> embryos at the cellular blastoderm stage (Fig. 6, a and b). Similar discrete T1/T2 and T2/T3 hybridization signals are detected in gastrulating P9/P9 embryos (Fig. 6, c and d).

In wild-type embryos undergoing retraction of the germ band, *Antp* transcripts are broadly distributed over the progenitors of the ventral cord. However, labeling of the presumptive abdominal ganglia is less intense as compared with future thoracic ganglia (Fig. 4, e and f). In contrast, P9/P9 embryos of this developmental stage show uniformly intense *Antp* hybridization signals from the future T1/T2 primordium posteriorly through A8 (Fig. 6, e and f).

**Patterns of ANT-C and BX-C gene expression in the CNS.** By mid-embryonic periods of development, each of the homeo box-containing homeotic genes of the ANT-C and BX-C comes to specify transcripts that appear to accumulate in largely discrete, nonoverlapping regions of the mature embryonic CNS (Fig. 7). The foci of transcript accumulation within the CNS seem to correspond to the embryonic segments that are most severely disrupted in mutants for the corresponding genes. During gastrulation and germ band extension, strong expression is also detected in epidermal and mesodermal tissues (Figs. 4, 5, and 6) (27, 29). By advanced stages of embryonic development, however, much of the

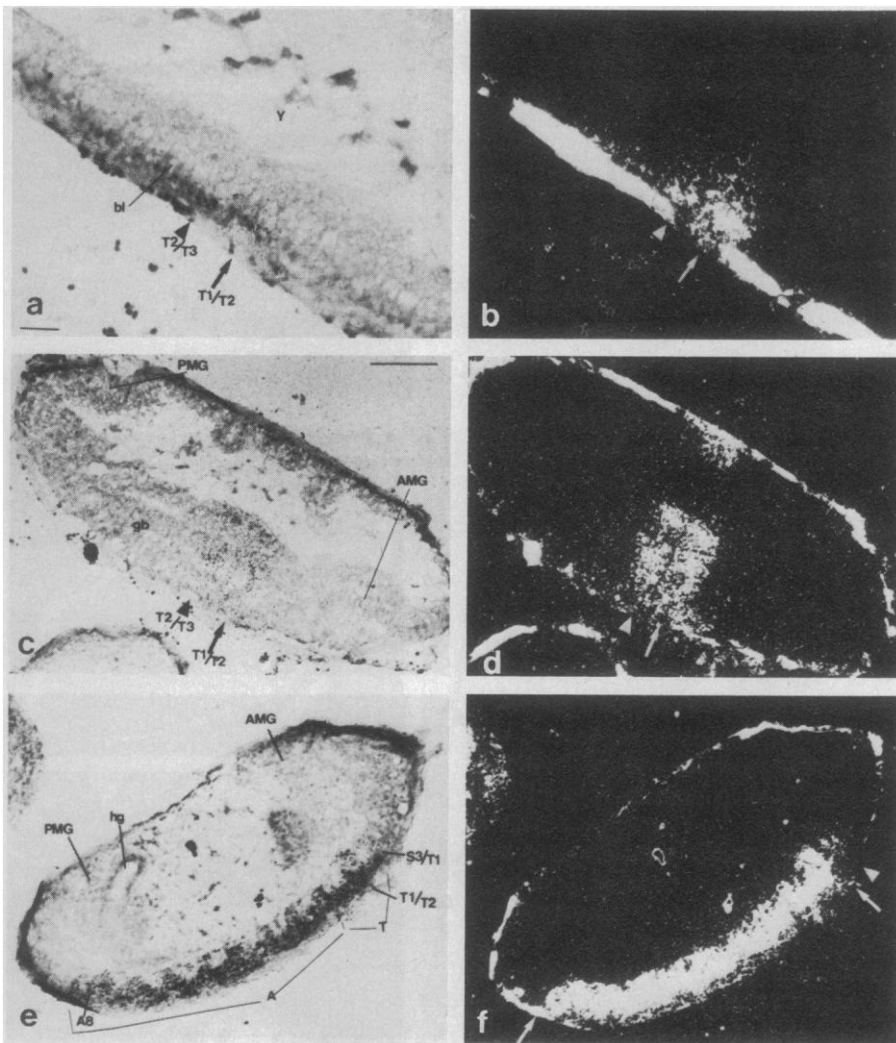


Fig. 6. Localization of *Antp* transcripts in BX-C<sup>-</sup> embryos. The orientation of the sections and other features are described in the legend to Fig. 3. Parallel sections through the same embryos did not show hybridization to either the *Ubx* or *iab-2* probes. (a) High magnification of a section through a BX-C<sup>-</sup> embryo at the cellular blastoderm stage; the bar represents 0.025 mm. Hybridization signals are seen over cells in the regions of the embryo which give rise to T1/T2 (arrow) and T2/T3 (arrowhead). (b) Dark-field photomicrograph of the same section as in (a). (c) A section through a gastrulating BX-C<sup>-</sup> embryo; bar indicates 0.1 mm. Hybridization signals are detected in regions giving rise to T1/T2 (arrow) and T2/T3 (arrowhead). (d) Dark-field photomicrograph of the same section as in (c). (e) A section through a BX-C<sup>-</sup> embryo undergoing germ band retraction. Uniformly intense signals are detected in T1/T2 through A8. Weaker signals are detected in cells of S3/T1. (f) Dark-field photomicrograph of the same section as in (e). Arrows demarcate T1/T2 to A8; the arrowhead indicates S3/T1 labeling. Abbreviations: A, abdominal region of the germ band; AMG, anterior midgut invagination; bl, blastoderm; hg, hindgut; PMG, posterior midgut invagination; T, thoracic region of the germ band.

labeling over the hypodermal and mesodermal tissues is no longer detectable. Because expression is seen to persist in the CNS over the course of embryonic and larval development, it serves as a convenient model for analyzing the spatial regulation of homeotic gene expression.

A striking feature of ANT-C and BX-C homeo box expression is the colinearity between the physical order of the genes within the chromosome and the embryonic segments where they are expressed along the body axis. Lewis first demonstrated such colinearity for the BX-C loci and their corresponding domains of function (5). The proximal-most (closest to the centromere) locus of the ANT-C that we have analyzed is *Dfd* (15). By mid-embryogenesis *Dfd* transcripts are principally detected in the anterior-most portion of the CNS that has been thus far shown to accumulate homeo box-containing transcripts (see Fig. 3). The *Scr* locus is distal to *Dfd* and transcripts homologous to the A40 clone accumulate in a region of the mature embryonic CNS that is just posterior to the *Dfd* domain. *Antp* transcripts are mostly confined to the T1/T2 region of the ventral cord. Similarly, the proximal-most BX-C homeo box region (*Ubx*) specifies the most anteriorly localized BX-C products within the CNS (T3/A1) (29). The more distal *iab-2* and *iab-7* loci specify transcripts that are detected primarily in ventral ganglia A1/A2 through A6/A7 and A6/A7 through A8/A9, respectively.

It has been suggested that diverse pathways of segment morphogenesis are established by different combinations of homeotic gene products (5, 35–37). In particular, Lewis has proposed that each embryonic segment primordium in the posterior half of the embryo contains a different combination of BX-C gene products (5, 38). According to the Lewis model there is a sequential activation of BX-C gene expression along the anterior-posterior axis of the embryo. Thus, the anterior-most segment anlage that is acted upon by the BX-C (T2p)(39) would contain products encoded by only one BX-C locus (*Ubx*), whereas the posterior-most segment primordium (A8) is expected to contain all BX-C gene products (*Ubx*, *iab-2*, and *iab-7*) (21).

During extension and retraction of the germ band, the transcript distribution patterns for the *Ubx*, *iab-2*, and *iab-7* loci are consistent with the Lewis model (see Fig. 5). Progenitors of the metathorax and first abdominal segment contain *Ubx* transcripts, but do not display detectable levels of either *iab-2* or *iab-7* transcripts. In contrast, progenitors of

the seventh (and possibly eighth) abdominal segment contain levels encoded by each of the homeo box-containing BX-C loci.

Over the course of embryonic development, there is a successive restriction in the spatial limits of transcript accumulation for at least some of the ANT-C and BX-C homeo box-containing loci. As compared with earlier periods of embryogenesis, advanced stage embryos show relatively discrete transcript accumulation patterns for each ANT-C and BX-C gene that contains a homeo box (compare Figs. 4 and 5 with Fig. 3).

While not specifically predicted by the Lewis model, this observation is consistent with the demonstration that each ANT-C and BX-C homeotic locus has a discrete primary domain of function (see Fig. 1a). For example, during germ band

extension, *Antp* transcripts are detected at almost uniform levels in the neural progenitors of segment primordia S3/T1 through A7/A8. In contrast, by late stages of embryogenesis, the T1/T2 ganglion cells display substantially stronger hybridization as compared with the ganglion cells of other segments. Thus, as embryogenesis proceeds, *Antp* becomes localized to the segments which are most disrupted by lethal mutations of the gene. It is therefore possible that the primary domain of function for a given homeotic gene is determined by the embryonic regions where its expression is sustained.

**Cross-regulatory interactions among homeo box genes.** It has been previously suggested that hierarchical interactions among homeotic genes might influence their spatially restricted domains of expression (35, 40). More recent evi-

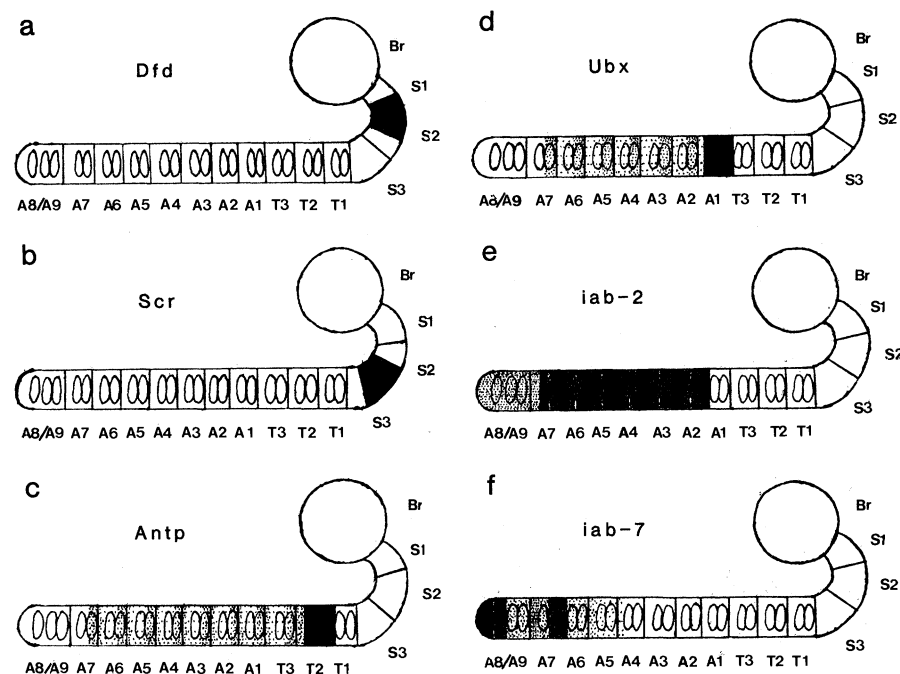


Fig. 7. Sites of ANT-C and BX-C expression in the embryonic CNS. The diagrams represent the CNS of a 14-hour embryo. The sites of *Dfd*, *Scr*, *Antp*, *Ubx*, *iab-2*, and *iab-7* transcript accumulation are indicated. Solid shading represents the strongest sites of hybridization for each probe. Stippled areas correspond to weaker levels of hybridization; the intensity of stippling represents qualitative but not quantitative differences in the extent of hybridization. Anterior is to the right, and dorsal is up. (a) *Dfd* transcripts appear to be localized to S1/S2. This assignment could be in error by half a segment; that is, the transcripts may be localized to S2. (b) Transcripts homologous to pA40 (*Scr*) are localized to S2/S3. Again, this assignment could be in error by half a segment; the transcripts could be localized to S3. (c) *Antp* transcripts accumulate most strongly in the posterior compartment of T1 (T1p) and the anterior compartment of T2 (T2a). Lower levels are detected, as indicated, through the anterior commissure of A7. (d) *Ubx* transcripts accumulate most strongly in T3p/A1a (29). Lower levels are seen posteriorly through the anterior commissure of A7. More transcripts are detected in ganglion cells associated with the anterior commissure of each of the A2 through A7 ganglia as compared with the posterior commissures (29, 42, 43). (e) *iab-2* transcripts accumulate strongly in A1p through A7a. There are probably more transcripts in the posterior compartment of each of the A2 through A6 ganglia than in the anterior compartment. Fewer transcripts are seen in A7p through A8/A9. (f) Transcripts homologous to *iab-7* accumulate strongly in A6p through A8/A9. However, labeling in this region is not uniform in that the A6p/A7a and A8p/A9 show higher levels of transcript than A7p/A8a. Fewer transcripts are seen anteriorly through at least A5a and possibly A4p. Abbreviations: Br, brain; S1, S2, S3, anterior, central, and posterior regions of the subesophageal ganglion, respectively; T1, prothoracic ganglion; T2, mesothoracic ganglion; T3, metathoracic ganglion; A1–A8, the first through eighth abdominal ganglia.

dence for such homeotic cross-regulatory interactions has been obtained by analysis of homeo box transcript distribution patterns in homeotic mutant embryos. *Antp* transcripts have been shown to stably accumulate in the posterior ventral ganglia of advanced stage embryos that lack all known genes of the BX-C. On this basis it was suggested that one or more BX-C gene products either directly or indirectly inhibit *Antp* expression (34). Here we present further support for this proposal.

The altered distribution of *Antp* transcripts in advanced stage BX-C<sup>-</sup> embryos could be either a direct or indirect consequence of deleting the BX-C. An example of an indirect effect is that the absence of the BX-C allows for the activation of *Antp* expression by a common trans-regulatory component that in wild-type embryos preferentially initiates BX-C gene expression. The data presented in Fig. 6 are not obviously consistent with this explanation. BX-C<sup>-</sup> embryos display a wild-type *Antp*<sup>+</sup> transcript distribution pattern during early developmental stages. Only after the sixth hour of embryogenesis do BX-C<sup>-</sup> individuals show a striking deviation from wild type in the *Antp*<sup>+</sup> transcript pattern. It is therefore unlikely that initiation of *Antp* expression is altered in BX-C<sup>-</sup> embryos. Thus, the altered *Antp*<sup>+</sup> pattern observed in Fig. 6, e and f, might result from the absence of products encoded by the BX-C rather than from the physical removal of the complex per se.

The molecular basis for possible cross-regulatory interactions among *Drosophila* homeotic loci is not known. Such interactions might be mediated by the different homeo box protein domains encoded by the various ANT-C and BX-C loci. There appears to be weak structural homology between the homeo domain and known (or suggested) DNA binding proteins (19, 41). It is possible that each homeo box-containing locus autoregulates its own expression, thereby permitting relatively high steady-state levels of product to accumulate within its primary domain of function. In contrast, homeo box-containing protein products might repress the expression of other homeo box-containing transcription units in a hierarchical manner. For example, perhaps *Antp* protein products act as positive regulators of *Antp* expression. This results in the maintenance of high levels

of *Antp* product within the primary domain of *Antp* function (that is, T1/T2 ventral ganglion cells). In embryonic ventral ganglia posterior to T1/T2, *Antp* product accumulation might be hindered by high affinity binding of BX-C homeo box-containing proteins to the *Antp* promoter. As a result, *Antp* products are observed to only transiently accumulate at high levels in the posterior ventral ganglia of wild-type embryos.

Consistent with this proposal is the demonstration that *Antp* RNA's stably accumulate in posterior portions of the developing ventral cord in embryos that lack all genes of the BX-C (34). Moreover, we have shown that the altered distribution of *Antp* transcript accumulation in BX-C<sup>-</sup> embryos probably does not result from initiation of *Antp* expression within inappropriate segment primordia (see Fig. 6). Rather, the absence of products encoded by one or more BX-C loci appears to be either directly or indirectly responsible for the stable accumulation of *Antp* transcripts in posterior ventral ganglia.

At present, there appears to be no direct evidence to support or reject this model of "homeo box competition" between different homeotic genes of the Antennapedia class. The availability of cloned homeotic DNA sequences and the isolation of proteins encoded by homeotic loci (42, 43) should furnish direct information regarding the spatial localization of homeotic gene products to discrete regions of developing embryos.

#### References and Notes

- G. F. Ferris, in *Biology of Drosophila*, M. Demerec, Ed. (Wiley, New York, 1950), pp. 368-419.
- P. A. Lawrence and P. Johnson, *Cell* **36**, 775 (1984).
- F. Jimenez and J. A. Campos-Ortega, *Arch. Entwicklungsmech. Org.* **190**, 370 (1981).
- D. R. Kankel, A. Ferrus, S. H. Garen, P. J. Harte, P. E. Lewis, in *The Genetics and Biology of Drosophila*, M. Ashburner and T. S. Wright, Eds. (Academic Press, New York, 1980), vol. 2, pp. 295-363.
- E. B. Lewis, *Nature (London)* **276**, 565 (1978).
- W. H. Ouweneel, *Adv. Genet.* **18**, 179 (1976).
- E. Teugels and A. Ghysen, *Nature (London)* **304**, 440 (1983).
- B. T. Wakimoto and T. C. Kaufman, *Dev. Biol.* **81**, 51 (1981).
- E. Sanchez-Herrero, I. Vernos, R. Marco, G. Morata, *Nature (London)* **313**, 108 (1985).
- R. E. Denell, *Genetics* **75**, 279 (1973).
- T. C. Kaufman, R. Lewis, B. Wakimoto, *ibid.* **94**, 115 (1980).
- E. B. Lewis, *Am. Zool.* **3**, 33 (1963).
- \_\_\_\_\_, in *Embryonic Development, Part A: Genetic Aspects* (Liss, New York, 1982), pp. 269-288.
- B. T. Wakimoto, F. R. Turner, T. C. Kaufman, *Dev. Biol.* **102**, 147 (1984).
- T. Hazelrigg and T. C. Kaufman, *Genetics* **105**, 581 (1983).

- W. McGinnis, M. S. Levine, E. Hafen, A. Kuroiwa, W. J. Gehring, *Nature (London)* **308**, 428 (1984).
- W. McGinnis, R. L. Garber, J. Wirz, A. Kuroiwa, W. J. Gehring, *Cell* **37**, 403 (1984).
- M. P. Scott and A. J. Weiner, *Proc. Natl. Acad. Sci. U.S.A.* **81**, 4115 (1984).
- A. Laughon and M. P. Scott, *Nature (London)* **310**, 25 (1984).
- M. Regulski, K. Harding, R. Kostriken, F. Karch, M. Levine, W. M. McGinnis, *Cell*, in press.
- In this report, we consider only the homeotic loci of the BX-C that contain a homeo box. There are additional homeotic loci within this complex (Fig. 1a), each of which has a well-defined domain of function (5). For example, a fly that lacks *bx* function shows a transformation of T3a into T2a. The Lewis model (see text) predicts that only *abx* and *bx* would be normally expressed in T3a but that all the loci of the BX-C would be expressed in A8.
- W. Bender *et al.*, *Science* **221**, 23 (1983).
- R. L. Garber, A. Kuroiwa, W. J. Gehring, *EMBO J.* **2**, 2027 (1983).
- M. P. Scott *et al.*, *Cell* **35**, 763 (1983).
- The molecular map positions of several *Dfd* mutant alleles indicate that the p99-5.0 probe (Fig. 1b) derives from the *Dfd* locus (M. Regulski and W. McGinnis, unpublished results).
- E. Hafen, M. Levine, R. L. Garber, W. J. Gehring, *EMBO J.* **2**, 617 (1983).
- M. Levine, E. Hafen, R. L. Garber, W. J. Gehring, *ibid.*, p. 2037.
- A. Kuroiwa and W. J. Gehring have localized the *Scr* locus region within overlapping cloned genomic DNA's that span most of the ANT-C (personal communication). On the basis of high stringency cross-hybridization tests with the cloned *Scr* DNA's it has been determined that A40 derives from the homeo box region of the *Scr* locus (W. McGinnis, A. Kuroiwa, W. J. Gehring, unpublished results).
- M. Akam, *EMBO J.* **2**, 2075 (1983).
- Our in situ localizations of transcripts could be in error by half a segment. The term "T1/T2" indicates that the region of hybridization could be in tissues of T1 or T2 (or both). Similarly, A1/A2, for example, indicates labeling in all or portions of the first or second abdominal ganglia (or both).
- D. F. Poulson, in *Biology of Drosophila*, M. Demerec, Ed. (Wiley, New York, 1950), pp. 168-274.
- I. Duncan, *Genetics* **100**, 520 (1981).
- G. Struhl, *J. Embryol. Exp. Morphol.* **76**, 297 (1983).
- E. Hafen, M. Levine, W. J. Gehring, *Nature (London)* **307**, 287 (1984).
- G. Struhl, *Proc. Natl. Acad. Sci. U.S.A.* **79**, 7380 (1982).
- A. Garcia-Bellido, *Am. Zool.* **17**, 613 (1977).
- \_\_\_\_\_, in *Cell Patterning*, S. Brenner, Ed. (Elsevier/North-Holland, Amsterdam, 1975), pp. 161-182.
- F. Karch *et al.*, in preparation.
- Each segment has two developmentally distinct subdivisions: an anterior and a posterior compartment (36, 37). The founder cells for each compartment are determined during early embryonic stages. The cells that give rise to one compartment do not intermix with those that give rise to the other. However, there are no overt morphological markers which delineate the compartments of a segment.
- G. Morata and S. Kerridge, *Nature (London)* **300**, 191 (1982).
- J. C. W. Shepherd, W. McGinnis, A. E. Carasco, M. DeRobertis, W. J. Gehring, *Nature (London)* **310**, 70 (1985).
- R. White and M. Wilcox, *Cell* **39**, 163 (1984).
- P. A. Beachy, S. L. Helfand, D. S. Hogness, *Nature (London)* **313**, 545 (1985).
- G. Struhl, *ibid.* **292**, 635 (1980).
- We thank Ernst Hafen, Eric Frei, and Markus Noll for stimulating and provocative discussions; Mark Dworkin, Eva Dworkin-Rastl, Ernst Hafen, Helen Doyle, Tim Hoey, and Lily Mirels for reviewing the manuscript; and Diane Robins for encouragement. This work was supported by a grant from the National Institutes of Health.

21 May 1985; accepted 2 August 1985